Available online at www.sciencedirect.com
SCIENCE DIRECT
International Journal of Mass Spectrometry 252 (2006) 213–221
International Journal of Mass Spectrometry
www.elsevier.com/locate/ijms

Ionization of W and W^+ by electron impact

Duck-Hee Kwon [a], Yong-Joo Rhee [a], Yong-Ki Kim [b,*]

[a] *Korea Atomic Energy Research Institute, Daejeon 305-600, South Korea*
[b] *National Institute of Standards, Gaithersburg, MD 20899, USA*

Received 19 January 2006; received in revised form 8 March 2006; accepted 8 March 2006
Available online 25 April 2006

Abstract

Theoretical cross-sections for electron-impact ionization of the neutral W atom and W^+ ion are reported. The direct ionization cross-sections were calculated by using the binary-encounter Bethe (BEB) model and the indirect ionization cross-sections resulting from numerous excitation-autoionization (EA) were calculated by using scaled Born cross-sections. Contributions to indirect ionization from spin-forbidden and $\Delta n = 1$ excitations, where n is the principal quantum number, are noticeable unlike in light atoms. The single ionization cross-section of W^+ is increased by about 10% due to the indirect EA of 5p electrons in the range of the incident electron energies between 40 and 60 eV. In the case of neutral W the EA cross-sections are very small for the $^7S_3$ level which is the first metastable term of W and because the excitations to the high spin states are mostly in the bound spectrum below the ionization limit. On the other hand, the EA cross-section of the second metastable ^3P term of W is large where a few $6s^2 \rightarrow 5d6p$ and many $5p \rightarrow 5d$, 6s excitations increase the total ionization cross-section by as much as 25%. Our total cross-section for the single ionization of W^+ is $\sim$ 15% higher at the peak than the two sets of experimental data available in the literature. Our cross-sections are compared to the scaled Born cross-sections derived from the formulas provided by McGuire and those derived from the semi-empirical formulas by Lotz.
Published by Elsevier B.V.

Keywords: Ionization cross-section; W, W^+; Autoionization

1. Introduction

Electron-impact ionization of tungsten (W, atomic number $Z = 74$) and tungsten ions have been investigated by some authors [1–3] because tungsten is a refractory material which will be used inside magnetic fusion devices such as tokamak. In spite of strong radiative loss of high-Z tungsten, the ASDEX (Axially Symmetric Divertor Experiment) Upgrade tokamak in Germany is designed to use tungsten facing in the divertor region to take advantage of very low sputtering rates of tungsten similar to the ITER (International Thermonuclear Experimental Reactor) plan. Therefore, electron-impact ionization cross-sections of tungsten and tungsten ions are essential data for divertor modeling. The ionization cross-section of singly charged tungsten ion (W^+) by electron impact was experimentally measured by two different groups, Montague and Harrison [1] and Stenke et al. [2]. However, the electron-impact ionization cross-section of neutral tungsten could not be measured because of low vapor pressure owing to the high melting point. The cross-section of W^+ measured by Montague and Harrison [1] was compared to the scaled Born prediction of McGuire [4]. McGuire's calculation is in good agreement with the measurement at higher incident electron energies over 100 eV but it underestimates the cross-section at energies below 100 eV. On the other hand the measured cross-section of W^+ by Stenke et al. [2] is lower than the configuration-average, distorted-wave Born (DWB) cross-section by Pindzola and Griffin [3] and the one-term Lotz formula [5]. Electron-impact ionization cross-section of the neutral atom was also calculated by Pindzola and Griffin [3] near the threshold using the DWB approximation. Their result shows however very different shape and peak position compared to the cross-section from the one-term Lotz formula [5].

We report in this article ionization cross-sections of neutral W and W^+ ion using the binary-encounter Bethe (BEB) model [6] for direct ionization of all electrons and scaled Born cross-section [7,8] for excitation-autoionization (EA) of outer-shell electrons. These methods have successfully been applied to Mo ($Z = 42$) and Mo^+ [9], which have half-filled 4d valence shell

* Corresponding author. Tel.: +1 301 975 3203; fax: +1 301 975 3038.
E-mail address: yong-ki.kim@nist.gov (Y.-K. Kim).

1387-3806/$ – see front matter. Published by Elsevier B.V.
doi:10.1016/j.ijms.2006.03.007

similar to W and W^+, as well as to light atoms such as B ($Z = 5$), C ($Z = 6$), N ($Z = 7$), O ($Z = 8$), Al ($Z = 13$), Ga ($Z = 31$) and In ($Z = 49$) [10,11]. We calculated total ionization cross-sections of W and W^+ for ground, first and second metastable levels individually and compared our results with experiments and theories by McGuire [4] and Lotz [5,12,13].

2. Theoretical procedure

Open shell atoms have two dominant processes contributing to ionization. The first is direct ionization caused by the ejection of bound electrons to continuum states. The second is indirect ionization through excitation-autoionization (EA) of outer-shell electrons into quasi-bound states above the lowest ionization limit. We used binary-encounter Bethe (BEB) model [6] for the direct ionization. The BEB cross-section for the direct ionization of electrons in an atomic orbital is given by

$$\sigma_{\text{neut}} = \frac{4\pi a_0^2 N R^2}{B^2[t + (u+1)/m]} \left[\frac{\ln t}{2} \left(1 - \frac{1}{t^2} \right) + 1 - \frac{1}{t} - \frac{\ln t}{t+1} \right], \tag{1}$$

for a neutral atom, and by

$$\sigma_{+} = \frac{4\pi a_0^2 N R^2}{B^2[t + (u+1)/2m]} \left[\frac{\ln t}{2} \left(1 - \frac{1}{t^2} \right) + 1 - \frac{1}{t} - \frac{\ln t}{t+1} \right], \tag{2}$$

for a singly charged ion. In Eqs. (1) and (2), a_0 is the Bohr radius, N the orbital electron occupation number, R the Rydberg energy, B the orbital binding energy, $t = T/B$ with the incident electron energy T, and $u = U/B$ with the orbital kinetic energy U. The constant m in the denominator is unity for K- and L-shell orbitals, and m = principal quantum number n of other orbitals.

The first logarithmic term in Eqs. (1) and (2) came from the leading part of the Bethe cross-section, the middle term, $1 - 1/t$, from the direct and pure exchange part of the Mott cross-section, and the last logarithmic term from the interference between the direct and exchange terms of the Mott cross-section. The total direct ionization cross-section is obtained by summing σ over all occupied orbitals. The denominator, $t + u + 1$, is a modification of the original plane-wave Born (PWB) and Mott cross-sections to emulate the increased flux of the incident electron resulting from its interaction with the target atom. Most collision theories, including the original PWB and Mott cross-sections, have only t in the denominator.

The factor m was introduced to avoid unrealistically small cross-sections resulting from increasing values of U as n increases for outer orbitals in heavy atoms. The introduction of the factor 2 in the denominator of Eq. (2) reflects the fact that the original Mott cross-section with only t in the denominator will eventually become accurate for highly charged ion targets. Both modifications have successfully been applied to molecules and molecular ions that contain heavy atoms [14].

Note that Eqs. (1) and (2) require data only from the initial bound states, which are far easier to calculate than properties that directly involve continuum states. Besides, Eqs. (1) and (2) are based on nonrelativistic theories and hence valid only for nonrelativistic T. We obtained the atomic data B, U and N of the initial bound state of target W and W^+ using relativistic wave functions from a multiconfiguration Dirac-Fock (MCDF) code [15].

Excitation-autoionization cross-sections were obtained using scaled PWB cross-sections for the neutral W and scaled Coulomb Born (CB) cross-sections for W^+. The unscaled PWB and CB approximations are based on the first-order perturbation theory and are reliable only at high T. Moreover, these approximations do not account for the electron exchange effect with the bound electrons in the target atom, the distortion of plane or Coulomb waves in the vicinity of the target atom, or the polarization of the target atom due to the presence of the incident electron. Hence, we adopted simple scaling methods called *BE scaling* [7] for PWB cross-sections and *E scaling* [8] for CB cross-sections as was done in the case of Mo and Mo^+ [9]. These scalings offer simple ways to correct the deficiencies of the Born approximations. These scalings can be used to modify the Born cross-sections at low T so that they become reliable at all T. The BE scaling is given by

$$\sigma_{\text{BE}} = \sigma_{\text{PWB}} \frac{T}{T + B + E}, \tag{3}$$

and the E scaling by

$$\sigma_{\text{E}} = \sigma_{\text{CB}} \frac{T}{T + E}, \tag{4}$$

where E is the excitation energy. Both the BE scaling and the E scaling have been verified to produce reliable results at low T for light as well as heavy atoms [7,8] even though the BE and E scaling cannot be derived from first principles. These scaling methods can be used for excitations to both low-lying (hence true bound) levels as well as highly excited (i.e., autoionizing) levels. However these scalings are valid only for electric dipole ($E1$)-*allowed, strong* excitations and cannot be used for weak processes such as $E1$-forbidden excitations because cross-sections for such weak transitions cannot be accurately described by the first-order Born approximation, particularly at low T. We included $E1$-allowed ($\Delta J = 0, \pm 1$), strong transitions with the oscillator strength $f > 0.05$ among many transitions to autoionizing levels above the lowest ionization limit.

In the calculation of CB cross-sections for W^+, the incident electron before and after the collision is represented by partial waves. The cross-sections for high T far from excitation thresholds do not easily converge because of the large number of partial waves needed. In order to obtain cross-sections valid for the entire range of T, we combined high-T PWB cross-sections, which can be represented by the Bethe approximation with constants α, β, and γ [16]:

$$\sigma_{\text{Bethe}}(T) = \frac{4\pi a_0^2}{T/R} \left[\alpha \ln \left(\frac{T}{R} \right) + \beta + \frac{\gamma R}{T} \right], \tag{5}$$

with the CB cross-sections near the thresholds by using a least squares fit with a four term polynomial with fitting constants b,

c and d:

$$\sigma_{CB}(T) = \frac{4\pi a_0^2}{T/R}\left[\alpha \ln\left(\frac{T}{R}\right) + b + \frac{cR}{T} + d\left(\frac{R}{T}\right)^2\right]. \quad (6)$$

In this way we were able to tabulate CB cross-sections for the entire range of T.

Many decades ago, Lotz proposed simple semi-empirical formulas for direct ionization of neutral atoms and atomic ions in a series of publications. Because of the simplicity of his formulas, his formulas are widely used among plasma modelers. The simplest, one-parameter formula is proposed in Ref. [5] with a note to use it for "four times and higher ionized ions". In spite of this warning, some researchers used this formula on ions with lower charge states (see for example, [2,3]) for the lack of alternatives. We compare this one-term Lotz formula with our cross-sections for W^+ using the same orbital binding energies and occupation numbers we used for our own theory in the next section.

Lotz also proposed a three-parameter formula for neutral atoms [12] to be used with the binding energies he tabulated [13]. His tabulated binding energies are not very accurate for heavy atoms. However, we used his binding energies for the neutral W since the parameters he chose are meant to be used with the binding energies he published. The cross-sections based on the three-term Lotz formula are compared to our cross-sections in Section 4. We used our orbital occupation numbers with the three-term Lotz formula. This allowed us to distinguish ground and metastable terms that have the same configuration. The Lotz formulas are only for direct ionization and cannot account for excitation-autoionization.

Similarly, McGuire published a collection of scaled Born cross-sections for heavy atoms and their ions [4] in the form of orbital cross-section tables. Again, we used his formulas with the orbital binding energies and occupation numbers we have used for our own results. The scaled Born cross-sections based on the McGuire formulas are compared to our results for both W^+ and W in the next two sections. Similar to the Lotz formulas, the McGuire formulas are only for direct ionization and cannot account for excitation-autoionization.

3. Cross-sections for W^+

We obtained direct ionization cross-sections of W^+ by using Eq. (2). Among the many metastable levels of W^+, we chose the $5d^5\,{}^6S_{5/2}$ level (0.920 eV above the ground level) as the lowest metastable term and the $5d^36s^2\,{}^4F_{3/2}$ (1.080 eV above the ground level) as the second metastable term. The cross-sections for the fine-structure levels in a given term are very close. The orbital constants for the ground level ($5d^46s\,{}^6D_{1/2}$) and the two metastable levels ($5d^5\,{}^6S_{5/2}$ and $5d^36s^2\,{}^4F_{3/2}$) are listed in Table A.1 in Appendix A. The orbital constants were calculated by using single configuration Dirac-Fock wave functions.

In the case of the ground level ($5d^46s\,{}^6D_{1/2}$) and the second metastable level $5d^36s^2\,{}^4F_{3/2}$, the 6s electron is ionized with the experimental ionization energy (IE) of 16.35 eV and $16.35 - 1.080 = 15.270$ eV, respectively, while for the first metastable level ($5d^5\,{}^6S_{5/2}$) the 5d electron is ionized with the experimental IE of $16.35 - 0.920 = 15.430$ eV. In all cases, the resulting W^{++} ion is in its ground term ($5d^4\,{}^5D$) or in one of the many metastable terms with the same configuration. We have assumed the W^{++} ions are statistically distributed in the five levels of the ^5D ground term. The center-of-gravity (c.g.) of the ^5D term is 0.7052 eV above the ground level $^5D_0$. We added this c.g. energy to the known IE of W^+, making the IE we used $16.35 + 0.7052 = 17.0552$ eV. We also added 0.7052 eV to the IE's of the two metastable W^+ levels. We replaced the theoretical binding energies of outermost electrons, i.e., 6s or 5d electrons, with the experimental IEs in Table A.1. The experimental energies of the ground and the metastable levels and the IEs are from the compiled energy levels of W^+ and W^{++} [17]. The noninteger occupation numbers for the $5d_{3/2}$ and $5d_{5/2}$ electrons resulted from distributing the nonrelativistic configuration $5d^3$, $5d^4$ or $5d^5$ among the combinations of relativistic configurations containing $5d_{3/2}$ and $5d_{5/2}$ electrons.

In order to obtain excitation-autoionization (EA) cross-sections of W^+ we considered only $E1$-allowed excitations of $6s \rightarrow 6p$, $5p \rightarrow 5d$ or 6s, and $5d \rightarrow 6p$ transitions whose f values exceeded 0.05 as was mentioned in Section 2. We excluded excitations of tightly bound inner-shell electrons such as 4p, 4d and 4f electrons because their large binding energies make their cross-sections very small. Among the above $E1$-allowed excitations those of 5p electrons are the only ones contributing to strong EA. We used MCDF wave functions with frozen configuration-average radial functions for the transitions of 5p electrons. We included the $5p^65d^46s$, $5p^65d^5$ and $5p^65d^36s^2$ configurations for the initial states of the $E1$ transition and $5p^55d^46s^2$, $5p^55d^56s$, and $5p^55d^6$ configurations for the final states. There were no strong transitions involving the 6p orbitals. Out of hundreds of transitions representing the $E1$-allowed excitations of the 5p electron, we found a total of 59 strong EA transitions for the ground and two metastable levels of W^+. Among them there were $\Delta n = 1$ transitions and spin-forbidden transitions ($\Delta S \neq 0$) indicating the breakdown of LS coupling as was the case for Mo and Mo^+ [9].

We calculated CB cross-sections for low T near the excitation thresholds and PWB cross-sections for T over 500 eV. Then, as was explained in Section 2, a polynomial was fitted to combine the CB cross-sections with the asymptotic PWB cross-sections. The E scaling shown in Eq. (4) was applied to the fitted equation. The calculated excitation energies were scaled by the ratio of the experimental and theoretical IE's to make the theoretical transition energies more realistic. Individual excitation energies may not be accurate, but we are confident that the sum of EA cross-sections will be realistic both in the range of excitation energies and magnitudes. We did not consider the branching ratio for photoemission versus autoionization assuming that all levels above the lowest IE decay by autoionization.

In this way total ionization cross-sections including the direct ionization and indirect excitation-autoionization are obtained and listed in Table A.2 in Appendix A for the ground and two metastable states of W^+. Single ionization represents the ionization of the 5d or 6s electrons, counting ionization stands for the ionization of all occupied electrons regardless of the final charge states of the ions produced, and gross ionization means the sum

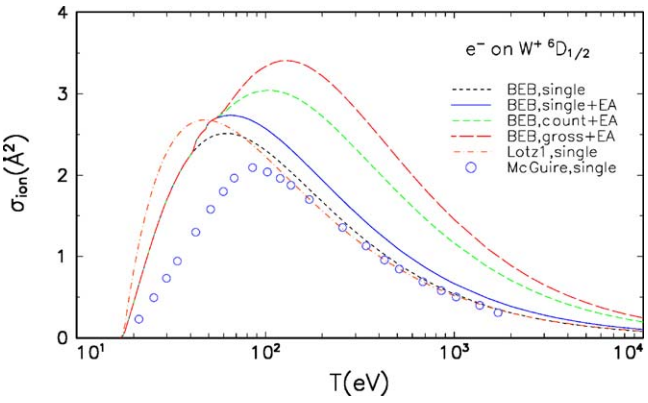

Fig. 1. Theoretical ionization cross-sections of W^+ in the $^6D_{1/2}$ ground level. Short dashed curve, present work for direct single ionization cross-section; solid curve, total single ionization cross-section including excitation-autoionization cross-sections; medium dashed curve, total counting ionization cross-section; long dashed curve, total gross ionization cross-section; dot dashed curve, one-term Lotz formula [5] for direct single ionization; circles, scaled Born cross-section by McGuire [4] for direct single ionization.

of ion current, i.e., doubly charged ions are recorded with the weight of two, triply charged ions with the weight of three, etc. Figs. 1–3 show the cross-sections for the $^6D_{1/2}$ ground, $^6S_{5/2}$, and $^4F_{3/2}$ metastable states respectively. The EA cross-sections contribute less than 10% to the total ionization cross-sections for the ground and two metastable states of W^+.

Single ionization cross-sections calculated from the one-term Lotz formula [5] and scaled Born cross-section from the McGuire formula [4] are compared to the present work in Figs. 1–3. As was mentioned in Section 2, we used our own ionization energies and orbital occupation numbers with the one-term Lotz and McGuire formulas for direct ionization. However, the Lotz and McGuire formulas do not include EA cross-sections. In spite of its simplicity, the one-term Lotz formula provides good cross-sections, while the McGuire formula consistently underestimates cross-sections between the ionization threshold and the cross-section peak for W^+.

Fig. 4 compares the single ionization cross-sections including EA cross-sections of the ground and two metastable levels with the experimental cross-sections. The peak ionization cross-sections of the ground $^6D_{1/2}$ and the first metastable $^6S_{5/2}$ levels

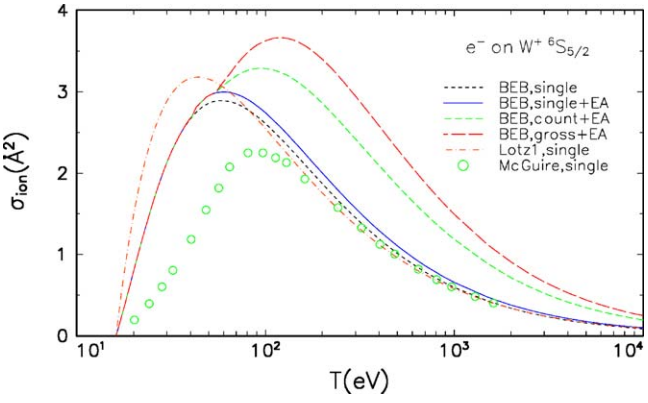

Fig. 2. Theoretical ionization cross-sections of W^+ in the $^6S_{5/2}$ metastable level. See the caption of Fig. 1 for legend.

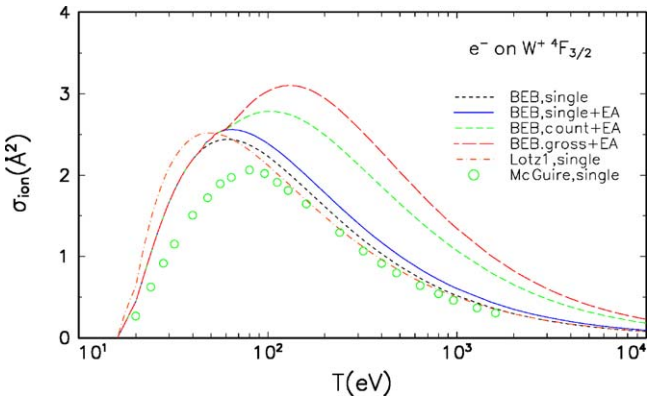

Fig. 3. Theoretical ionization cross-sections of W^+ in the $^4F_{3/2}$ metastable level. See the caption of Fig. 1 for legend.

are higher than the two experimental values. The total ionization cross-section of the second metastable $^4F_{3/2}$ level looks closest to the experimental cross-sections but a little higher in the peak value than the experiments. A mixture of 70% $^6S_{5/2}$ and 15% $^4F_{3/2}$ of W^+ target beam reproduces the shape and the magnitude of the experimental cross-sections well. Moreover, the threshold behavior of experimental data clearly indicates that the target W^+ beam contained a substantial amount of metastable W^+ ions. The experimental data in Fig. 4 start to rise from $T < 16$ eV, which is closer to the IEs of the two metastable states than that of the ground state of W^+.

We also calculated the direct ionization cross-section of the third metastable term of W^+, $5d^46s\,^4D$, but obtained even a higher peak cross-section than the ones we presented in Fig. 4. Hence, higher metastable terms are not likely to be the cause for the $\sim$ 15% difference in the theoretical and experimental peak values seen in Fig. 4. The DWB cross-section [3] for the (direct) ionization of W^+ peaks near $T = 50$ eV with a peak value of about 4 Å^2.

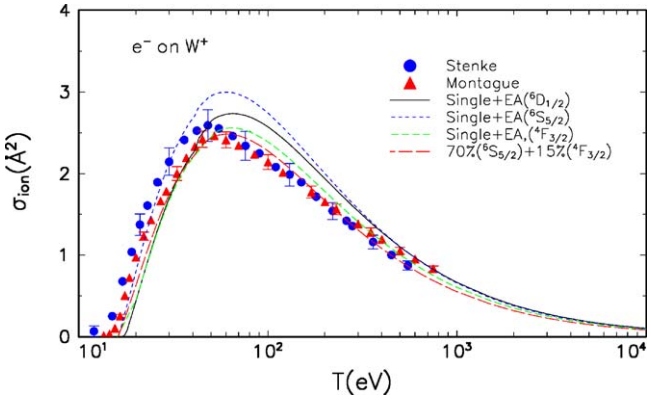

Fig. 4. Comparison of the present work to experimental single ionization cross-sections of W^+. Solid curve, total single ionization cross-section for the ground level $^6D_{1/2}$; short dashed curve, total single ionization cross-section for the metastable level $^6S_{5/2}$; medium dashed curve, total single ionization cross-section for the metastable level $^4F_{3/2}$; long-dashed curve, total single ionization cross-section for a mixture of 70% $^6S_{5/2}$ metastable ions and 15% $^4F_{3/2}$ metastable ions; circles, experimental data by Stenke et al. [2]; triangles, experimental data by Montague and Harrison [1].

4. Cross-sections for W

For the neutral W atom, we calculated ionization cross-sections for the ground level, $5d^4 6s^2\ ^5D_0$, and two metastable levels, $5d^5 6s\ ^7S_3$ and $5d^4 6s^2\ ^3P_1$. The direct ionization cross-sections were calculated using Eq. (1). As was mentioned in Section 3 the cross-sections for the members of a fine-structure multiplet are very similar. The 6s electron is ionized in the cases of the ground level and the second metastable W producing W^+ in the ground term, $5d^4 6s\ ^6D$. Ionization of the 6s electron from the first metastable level $5d^5 6s\ ^7S_3$ of W will result in a metastable W^+ ion in the $5d^5\ ^6S$ term, while ionization of a $5d_{3/2}$ or $5d_{5/2}$ electron will produce a W^+ ion in the ground configuration, $5d^4 6s$. Hence, for the $^7S_3$ metastable level of W, we assumed that either a $5d_{3/2}$ or $5d_{5/2}$ electron is ionized with the IE of $7.864 - 0.366 + 0.514 = 8.012$ eV, although the calculated binding energies are 8.48 eV for the $5d_{3/2}$ electron and 8.23 eV for the $5d_{5/2}$ electron. From the compiled energy levels of W and W^+ [17], we find that the IE of the ground level $^5D_0$ is 7.864 eV, the IE of the first metastable level $^7S_3$ is 7.498 eV and the IE of the second metastable level $^3P_1$ is $7.864 - 1.6499 = 6.2141$ eV. As in the case of W^+, we added the center of gravity (0.5138 eV) for the ground ^6D term of W^+ to the IEs of all three levels of W.

The orbital constants for the ground and metastable levels of W are listed in Table A.3 in Appendix A. We used configuration mixing between $5d^4 6s^2$ and $5d^5 6s$ because the levels are significantly mixed with the configurations as clearly shown in the occupation numbers of $5d_{3/2}$, $5d_{5/2}$ and 6s orbitals for the ground and the second metastable levels displayed in Table A.3. The single, counting and gross ionization cross-sections including EA cross-sections for the ground and two metastable levels are listed in Table A.4 in Appendix A.

Significant contributions to the indirect ionization of W come from the EA of the $6s \rightarrow 6p$ and $5p \rightarrow 5d$, 6s excitations. As in the case of W^+, we retained only $E1$-allowed excitations with $f > 0.05$. Some autoionizing excitations correspond to the $6s^2 \rightarrow 5d6p$ excitations while there are no significant contributions from this type of excitations in W^+. Excitations of the type $6s^2 \rightarrow 5d6p$ significantly contribute to indirect ionization at low T for the ground ^5D term and the second metastable ^3P term, but not to the first metastable ^7S term. A similar trend was also observed in the case of Mo [9].

As was done for W^+, we used configuration-average radial functions to calculate autoionizing states to be included in the indirect ionization. The excitation energies of the selected levels were scaled by the ratio of the calculated and known experimental IE's to make the excitation energies more realistic. As was explained in Section 2, BE-scaled PWB cross-sections [Eq. (3)] were used to calculate EA cross-sections. In reality some of the 5p-excited levels may decay by photoemission, and hence not produce an ion. The evaluation of the branching ratios for photoemission versus autoionization is a major theoretical undertaking beyond the scope of the present study. We have assumed that all 5p hole states decay by autoionization since autoionization is still a dominant process for excitation energies much less than 100 eV. We included a total of 96 autoionizing excitations.

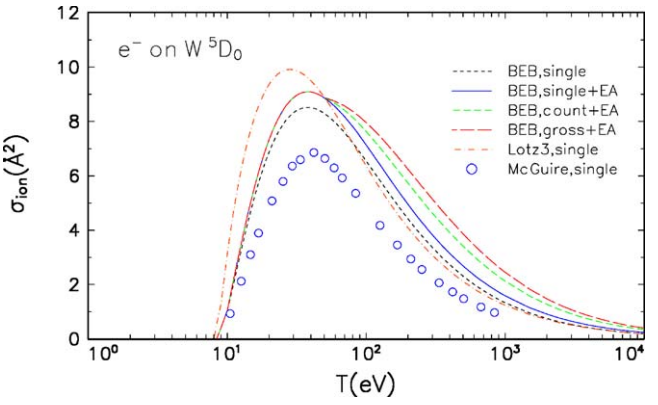

Fig. 5. Theoretical ionization cross-sections of W in the $^5D_0$ ground level. Short dashed curve, present work for direct single ionization cross-section; solid curve, total single ionization cross-section including excitation-autoionization cross-sections; medium dashed curve, total counting ionization cross-section; long dashed curve, total gross ionization cross-section; dot dashed curve, three-term Lotz formula [12] for direct single ionization; circles, scaled Born cross-section by McGuire [4] for direct single ionization.

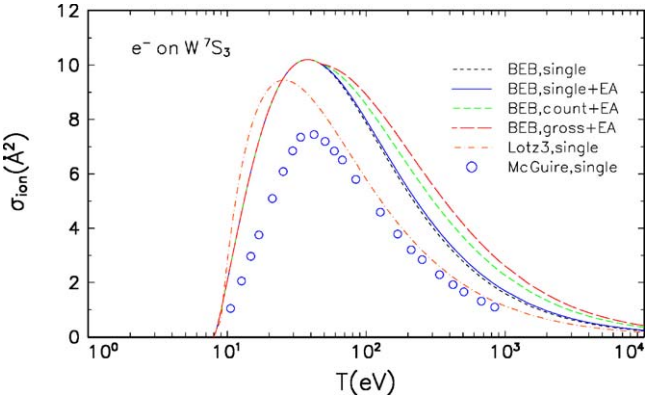

Fig. 6. Theoretical ionization cross-sections of W in the $^7S_3$ metastable level. See the caption of Fig. 5 for legend.

The total single, counting, and gross ionization cross-sections including the sum of EA cross-sections for each initial level of W are shown in Figs. 5–7. In Fig. 8 we compare the total single ionization cross-sections of the ground and two metastable states.

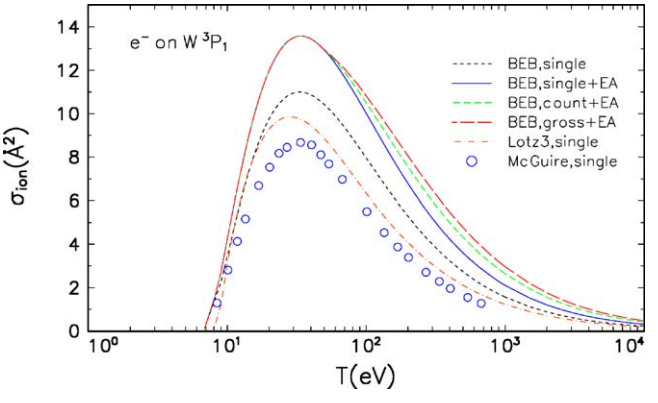

Fig. 7. Theoretical ionization cross-sections of W in the $^3P_1$ metastable level. See the caption of Fig. 5 for legend.

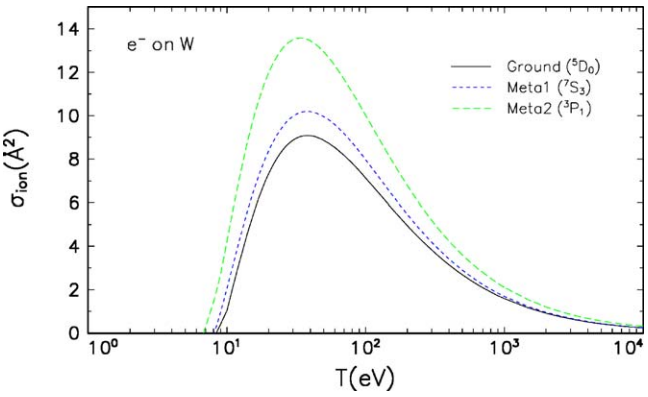

Fig. 8. Theoretical total single ionization cross-sections of W. Solid curve, present work for the ionization of the ground level $^5D_0$; short dashed curve, for the ionization of the metastable level $^7S_3$; long dashed curve, for the ionization of the metastable level $^3P_1$.

Except for the cross-section for the ground level of W, the three-term Lotz formula [12] tends to produce smaller cross-sections than our results, while the McGuire formula [4] underestimates cross-sections at all T for the neutral W atom.

5. Conclusions

We applied to W and W^+ a combination of the BEB model for the direct ionization and the BE and E scaling of the plane-wave and Coulomb Born cross-sections for the indirect ionization through excitation-autoionization.

The calculated single ionization cross-sections of W^+ show different behaviors for the ground and lowest metastable terms. The cross-sections of the ground and the first lowest metastable term are much higher in peak than the experimental cross-sections by Montague and Harrison [1] and Stenke et al. [2]. The cross-section peak of the second metastable term is very close to the experimental cross-sections. A combination of the cross-sections for a mixture of 70% $^6S_{5/2}$ (the first metastable level) ions and 15% $^4F_{3/2}$ (the second metastable level) ions reproduces the shape and magnitude of the experiments well. Also the experimental thresholds where the experimental ionization cross-sections start to rise are closer to the IEs of the two metastable terms rather than the IE of the ground term. Hence, the W^+ ions used in both experiments may have been mostly in metastable levels. The EA cross-sections of W^+ resulting from the 5p excitations contribute less than 10% to the total single ionization similar to the case of Mo^+ [9].

In the case of neutral W atom the first metastable ^7S term is not much affected by EA because excited states with high spin lie mostly below the ionization limit while the ground ^5D and the second metastable ^3P terms are substantially affected by EA. In particular the EA cross-sections of the second metastable term raise the peak value of the total ionization cross-section by about 25%. These trends were also seen in the case of neutral Mo [9].

According to Pindzola and Griffin [3], the DWB cross-section for W they calculated has a huge shape resonance near the ionization threshold reaching a peak cross-section of about 24 Å^2. This peak is located near $T = 10$ eV. They also show the one-term Lotz formula [5] for W to reach ~ 13 Å^2 near $T = 17$ eV without any resonance, while their DWB cross-section for single ionization reduces to about 17 Å^2 excluding any EA contribution. As is the case for the Lotz formula, the BEB model we have used is too simple to describe resonances although we have used a far better description of the target than those used in the Lotz formula or by Pindzola and Griffin in their DWB calculation. Since the DWB approximation is not expected to be reliable at such a low T, the actual location and the size of the shape resonance are likely to be substantially different from the prediction by Pindzola and Griffin [3].

The DWB cross-section for the single ionization of W^+ reported also by Pindzola and Griffin [3] peaks near $T = 50$ eV with a peak value of ~ 4 Å^2. Their DWB cross-section is for direct ionization only. This is to be compared to our peak cross-sections of ~ 3 Å^2 or less (Fig. 4). Our cross-sections include direct ionization and contributions from excitation-autoionization.

Unlike the one-term Lotz formula used by Pindzola and Griffin for the neutral W atom, the three-term Lotz formula [12] recommended by Lotz for neutral atoms provides more reasonable direct ionization cross-sections as shown in Figs. 5–7. On the other hand, the scaled Born cross-sections calculated from the McGuire formula [4] are consistently smaller than our results for both W and W^+.

Figs. 1–3 and 5–7 clearly demonstrate that the Lotz and McGuire cross-sections have different shapes and peak values than the direct ionization cross-sections calculated from the BEB model. The total ionization cross-sections obtained by adding our EA cross-sections to the direct ionization cross-sections from the Lotz or McGuire formulas would not agree well with the experimental data in Fig. 4, because the direct ionization cross-section is the dominant part of the total ionization cross-section.

With the results for W and W^+ presented here, we conclude that our theoretical method for calculating total ionization cross-sections of light and heavy atoms with open valence shells offers practical and reliable solutions. Even though the peak of our calculated cross-section for W^+ is about 15% higher than the experiments the shape is reproduced well by a combination of the cross-sections for the two lowest metastable terms. Moreover, the peak of the cross-section for W^+ calculated by our method is much closer to the experiments than the scaled Born cross-section calculated from the McGuire formula [4] and one-term Lotz formula [5]. We found that the cross-sections of neutral W and W^+ behave qualitatively similar to those of neutral Mo and Mo^+ [9].

Acknowledgements

We are deeply indebted to Dr. J.P. Desclaux and Dr. P. Indelicato for providing us with their latest multiconfiguration Dirac-Fock code and to Dr. A.E. Kramida for compiled energy levels of W, W^+, and W^{++}. The work at NIST was supported in part by the Office of Fusion Sciences of the United States Department of Energy. The work at KAERI was supported in part by Korea Basic Science Institute.

Appendix A

See Tables A.1–A.4.

Table A.1
Orbital binding energy B, kinetic energy U, and electron occupation number N for the ground and two metastable levels of W^+

Orbital[a]	$^6D_{1/2}$			$^6S_{5/2}$			$^4F_{3/2}$		
	B (eV)	U (eV)	N[b]	B (eV)	U (eV)	N[b]	B (eV)	U (eV)	N[b]
1s	69745.22	86797.79	2	69742.42	86797.87	2	69748.40	86797.71	2
2s	12194.29	20075.65	2	12191.35	20075.58	2	12197.61	20075.73	2
2p*	11617.46	19962.14	2	11614.52	19962.26	2	11620.77	19962.09	2
2p	10276.67	16561.25	4	10273.78	16561.24	4	10279.96	16561.27	4
3s	2876.58	6473.52	2	2873.64	6473.25	2	2879.88	6473.78	2
3p*	2624.99	6353.70	2	2622.07	6353.61	2	2628.28	6353.81	2
3p	2330.37	5498.80	4	2327.47	5498.67	4	2333.65	5498.91	4
3d*	1919.56	5337.38	4	1916.62	5337.17	4	1922.85	5337.45	4
3d	1856.61	5133.31	6	1853.74	5133.47	6	1859.87	5133.25	6
4s	631.30	2056.86	2	628.35	2056.50	2	634.63	2057.24	2
4p*	526.63	1946.69	2	523.67	1946.55	2	529.93	1946.65	2
4p	457.57	1691.49	4	454.67	1691.87	4	460.85	1691.20	4
4d*	287.11	1482.00	4	284.12	1481.87	4	290.41	1481.51	4
4d	274.05	1417.25	6	271.23	1418.40	6	277.29	1416.56	6
4f*	58.41	1011.92	6	55.45	1012.81	6	61.71	1012.21	6
4f	55.96	991.63	8	53.09	990.01	8	59.23	992.66	8
5s	100.70	429.24	2	97.73	422.87	2	103.96	432.33	2
5p*	67.99	349.54	2	64.72	347.67	2	71.08	353.52	2
5p	56.28	294.55	4	54.21	289.43	4	58.91	299.26	4
5d*	17.82	137.46	2.6382	16.14[c]	129.91	2.3059	20.07	150.17	2.4006
5d	17.52	128.70	1.3618	16.14[c]	121.46	2.6941	19.90	142.64	0.5994
6s	17.06[c]	54.51	1				15.98[c]	54.83	2

[a] Notation: $nl^* = nl_{j=l-1/2}$, $nl = nl_{j=l+1/2}$.
[b] The noninteger occupation numbers for the $5d_{3/2}$ and $5d_{5/2}$ electrons resulted from distributing the nonrelativistic 5d electron among the combinations of relativistic configurations containing $5d_{3/2}$ and $5d_{5/2}$ electrons.
[c] Experimental values from Ref. [17].

Table A.2
Cross-sections of W^+ in the ground and metastable levels for single ionization σ_{singl}, counting ionization σ_{cnt}, and gross ionization σ_{grs} as a function of incident electron energy T

T (eV)	$^6D_{1/2}$			$^6S_{5/2}$			$^4F_{3/2}$		
	σ_{singl}	σ_{cnt}	σ_{grs}	σ_{singl}	σ_{cnt}	σ_{grs}	σ_{singl}	σ_{cnt}	σ_{grs}
15.975							0	0	0
16.135				0	0	0	0.0187	0.0187	0.0187
16.500				0.0760	0.0760	0.0760	0.0616	0.0616	0.0616
17.055	0	0	0	0.1934	0.1934	0.1934	0.1268	0.1268	0.1268
17.5	0.0217	0.0217	0.0217	0.2878	0.2878	0.2878	0.1785	0.1785	0.1785
18.0	0.0825	0.0825	0.0825	0.3934	0.3934	0.3934	0.2356	0.2356	0.2356
18.5	0.1711	0.1711	0.1711	0.4977	0.4977	0.4977	0.2913	0.2913	0.2913
19	0.2597	0.2597	0.2597	0.6000	0.6000	0.6000	0.3452	0.3452	0.3452
20	0.4345	0.4345	0.4345	0.7972	0.7972	0.7972	0.4489	0.4489	0.4489
25	1.1836	1.1836	1.1836	1.6016	1.6016	1.6016	1.1675	1.1675	1.1675
30	1.6975	1.6975	1.6975	2.1293	2.1293	2.1293	1.6654	1.6654	1.6654
40	2.2445	2.2445	2.2445	2.6745	2.6745	2.6745	2.1920	2.1920	2.1920
50	2.6427	2.6427	2.6427	2.9509	2.9509	2.9509	2.4448	2.4448	2.4448
60	2.7272	2.7677	2.7895	2.9983	3.0803	3.1256	2.5545	2.5619	2.5663
70	2.7298	2.8949	2.9944	2.9704	3.1944	3.3297	2.5507	2.6614	2.7280
80	2.6931	2.9791	3.1570	2.9066	3.2597	3.4787	2.5106	2.7316	2.8694
90	2.6363	3.0234	3.2664	2.8261	3.2851	3.5719	2.4526	2.7692	2.9688
100	2.5697	3.0391	3.3345	2.7389	3.2839	3.6257	2.3863	2.7820	3.0322
120	2.4274	3.0241	3.4021	2.5635	3.2387	3.6649	2.2474	2.7661	3.0958
140	2.2883	2.9682	3.3994	2.3992	3.1576	3.6367	2.1137	2.7152	3.0981
165	2.1288	2.8717	3.3422	2.2161	3.0359	3.5531	1.9619	2.6277	3.0511

Table A.2 (*Continued*)

T (eV)	$^6D_{1/2}$			$^6S_{5/2}$			$^4F_{3/2}$		
	σ_{singl}	σ_{cnt}	σ_{grs}	σ_{singl}	σ_{cnt}	σ_{grs}	σ_{singl}	σ_{cnt}	σ_{grs}
180	2.0418	2.8078	3.2925	2.1179	2.9595	3.4898	1.8796	2.5698	3.0082
200	1.9356	2.7209	3.2168	1.9994	2.8583	3.3984	1.7795	2.4909	2.9419
250	1.7125	2.5106	3.0121	1.7545	2.6209	3.1631	1.5706	2.2999	2.7600
300	1.5369	2.3238	2.8151	1.5649	2.4155	2.9443	1.4070	2.1297	2.5829
400	1.2795	2.0229	2.4793	1.2915	2.0903	2.5789	1.1686	1.8560	2.2795
500	1.1003	1.7924	2.2118	1.1038	1.8448	2.2926	1.0033	1.6458	2.0364
600	0.9680	1.6118	1.9978	0.9666	1.6543	2.0655	0.8816	1.4810	1.8413
700	0.8661	1.4665	1.8234	0.8617	1.5019	1.8815	0.7881	1.3482	1.6819
800	0.7850	1.3470	1.6785	0.7787	1.3771	1.7294	0.7137	1.2389	1.5493
900	0.7188	1.2468	1.5564	0.7113	1.2728	1.6015	0.6532	1.1471	1.4372
1000	0.6637	1.1615	1.4519	0.6553	1.1843	1.4924	0.6028	1.0690	1.3413
1500	0.4845	0.8725	1.0951	0.4749	0.8860	1.1217	0.4393	0.8039	1.0131
2000	0.3851	0.7046	0.8861	0.3758	0.7138	0.9056	0.3488	0.6495	0.8204
3000	0.2768	0.5154	0.6493	0.2685	0.5204	0.6618	0.2503	0.4753	0.6016
4000	0.2180	0.4100	0.5170	0.2107	0.4132	0.5261	0.1971	0.3783	0.4792
5000	0.1809	0.3422	0.4317	0.1743	0.3445	0.4388	0.1633	0.3158	0.4003

All cross-sections are in $Å^2$.

Table A.3
Orbital binding energy B, kinetic energy U, and electron occupation number N for the ground and metastable levels of W

Orbital[a]	$^5D_0$			$^7S_3$			$^3P_1$		
	B (eV)	U (eV)	N[b]	B (eV)	U (eV)	N[b]	B (eV)	U (eV)	N[b]
1s	69966.84	86976.22	2	69964.42	86976.26	2	69967.19	86976.21	2
2s	12211.71	20091.20	2	12209.19	20091.18	2	12212.05	20091.23	2
2p*	11651.88	20034.19	2	11649.33	20034.35	2	11652.18	20034.30	2
2p	10296.27	16614.62	4	10293.80	16614.59	4	10296.64	16614.60	4
3s	2873.57	6479.43	2	2871.04	6479.30	2	2873.89	6479.46	2
3p*	2625.29	6371.53	2	2622.77	6371.50	2	2625.60	6371.58	2
3p	2327.61	5510.98	4	2325.11	5510.88	4	2327.94	5510.97	4
3d*	1915.39	5346.98	4	1912.83	5346.68	4	1915.67	5346.75	4
3d	1851.19	5141.19	6	1848.73	5141.43	6	1851.55	5141.36	6
4s	624.72	2059.75	2	622.18	2059.51	2	625.04	2059.75	2
4p*	520.74	1952.55	2	518.15	1952.25	2	521.01	1952.23	2
4p	450.92	1694.97	4	448.42	1695.30	4	451.26	1695.08	4
4d*	280.06	1484.51	4	277.41	1483.91	4	280.27	1483.42	4
4d	266.69	1418.50	6	264.28	1419.61	6	267.08	1418.82	6
4f*	50.79	1011.51	2	48.20	1013.22	2	51.06	1013.25	2
4f	48.22	991.29	2	45.75	989.53	2	48.57	990.36	2
5s	92.97	444.21	4	90.79	427.87	4	93.48	439.31	4
5p*	60.90	349.65	6	57.61	350.03	6	60.38	352.88	6
5p	48.74	294.70	8	47.03	290.31	8	49.36	294.24	8
5d*	10.09	132.87	2.9183	8.01[c]	121.46	2.2567	9.60	132.40	2.1138
5d	10.08	123.30	1.1211	8.01[c]	112.07	2.7432	8.79	118.99	1.9919
6s	8.38[c]	25.87	1.9606	8.42[c]	42.26	1.0000	6.73[c]	32.64	1.8944

[a] Notation: $nl^* = nl_{j=l-1/2}$, $nl = nl_{j=l+1/2}$.
[b] The noninteger occupation numbers for the $5d_{3/2}$, $5d_{5/2}$, and 6s electrons resulted both from the configuration mixing among nonrelativistic configurations $5d^46s^2$ and $5d^56s$ and from distributing the nonrelativistic 5d electron among the combinations of relativistic configurations containing $5d_{3/2}$ and $5d_{5/2}$ electrons.
[c] Experimental values from Ref. [17].

Table A.4
Cross-sections of W in the ground and metastable levels for single ionization σ_{singl}, counting ionization σ_{cnt}, and gross ionization σ_{grs} as a function of incident electron energy T

T (eV)	$^5D_0$			$^7S_3$			$^3P_1$		
	σ_{singl}	σ_{cnt}	σ_{grs}	σ_{singl}	σ_{cnt}	σ_{grs}	σ_{singl}	σ_{cnt}	σ_{grs}
6.728							0	0	0
7.000							0.2834	0.2834	0.2834
8.000							1.4300	1.4300	1.4300
8.012				0	0	0	1.4427	1.4427	1.4427
8.378	0	0	0	0.2907	0.2907	0.2907	1.9150	1.9150	1.9150
9	0.4082	0.4082	0.4082	0.9680	0.9680	0.9680	2.7248	2.7248	2.7248
10	1.0473	1.0473	1.0473	2.0712	2.0712	2.0712	4.2515	4.2515	4.2515
12	3.0237	3.0237	3.0237	4.0352	4.0352	4.0352	6.8189	6.8189	6.8189
14	4.5666	4.5666	4.5666	5.5905	5.5905	5.5905	8.7636	8.7636	8.7636
16	5.7550	5.7550	5.7550	6.7856	6.7856	6.7856	10.1875	10.1875	10.1875
18	6.6567	6.6567	6.6567	7.6966	7.6966	7.6966	11.2307	11.2307	11.2307
20	7.3377	7.3377	7.3377	8.3893	8.3893	8.3893	11.9918	11.9918	11.9918
25	8.3879	8.3879	8.3879	9.4698	9.4698	9.4698	13.0872	13.0872	13.0872
30	8.8769	8.8769	8.8769	9.9794	9.9794	9.9794	13.5065	13.5065	13.5065
35	9.0630	9.0630	9.0630	10.1734	10.1734	10.1734	13.5729	13.5729	13.5729
40	9.0790	9.0790	9.0790	10.1866	10.1866	10.1866	13.4486	13.4486	13.4486
45	8.9971	8.9971	8.9971	10.0941	10.0941	10.0941	13.2202	13.2202	13.2202
50	8.8587	8.8713	8.8772	9.9513	9.9903	10.0109	12.9362	12.9443	12.9472
60	8.5228	8.6470	8.7247	9.5830	9.7519	9.8576	12.3024	12.4191	12.4914
70	8.1615	8.4024	8.5591	9.1646	9.4606	9.6526	11.6704	11.9033	12.0545
80	7.7992	8.1410	8.3658	8.7456	9.1481	9.4119	11.0734	11.4065	11.6254
90	7.4527	7.8780	8.1584	8.3450	8.8346	9.1562	10.5219	10.9381	11.2124
100	7.1281	7.6244	7.9524	7.9699	8.5339	8.9055	10.0164	10.5032	10.8247
120	6.5483	7.1533	7.5536	7.3005	7.9758	8.4212	9.1332	9.7283	10.1221
140	6.0533	6.7317	7.1797	6.7299	7.4794	7.9726	8.3945	9.0630	9.5045
165	5.5328	6.2700	6.7549	6.1314	6.9393	7.4687	7.6299	8.3574	8.8359
200	4.9448	5.7261	6.2367	5.4574	6.3077	6.8612	6.7784	7.5504	8.0549
250	4.3043	5.1064	5.6259	4.7267	5.5944	6.1542	5.8641	6.6574	7.1713
300	3.8208	4.6207	5.1338	4.1780	5.0401	5.5909	5.1820	5.9735	6.4814
400	3.1372	3.9063	4.3901	3.4072	4.2320	4.7490	4.2283	4.9900	5.4692
500	2.6746	3.4008	3.8509	2.8896	3.6661	4.1458	3.5899	4.3094	4.7555
600	2.3391	3.0222	3.4403	2.5166	3.2453	3.6902	3.1301	3.8071	4.2217
700	2.0837	2.7264	3.1159	2.2340	2.9186	3.3325	2.7820	3.4191	3.8054
800	1.8822	2.4881	2.8523	2.0121	2.6567	3.0433	2.5084	3.1092	3.4704
900	1.7189	2.2915	2.6333	1.8327	2.4414	2.8040	2.2873	2.8551	3.1942
1000	1.5835	2.1261	2.4481	1.6846	2.2610	2.6023	2.1046	2.6428	2.9622
1500	1.1475	1.5778	1.8281	1.2110	1.6668	1.9316	1.5191	1.9460	2.1944
2000	0.9085	1.2660	1.4717	0.9536	1.3318	1.5492	1.1999	1.5548	1.7589
3000	0.6498	0.9194	1.0724	0.6773	0.9621	1.1235	0.8561	1.1237	1.2756
4000	0.5105	0.7285	0.8512	0.5297	0.7597	0.8891	0.6717	0.8881	1.0100
5000	0.4227	0.6065	0.7094	0.4371	0.6309	0.7394	0.5557	0.7382	0.8404

All cross-sections are in $Å^2$.

References

[1] R.G. Montague, M.F.A. Harrison, J. Phys. B 17 (1984) 2707.
[2] M. Stenke, K. Aichele, G. Hofmann, M. Steidl, R. Völpel, E. Salzborn, J. Phys. B 28 (1995) 2711.
[3] M.S. Pindzola, D.C. Griffin, Phys. Rev. A 46 (1992) 2486.
[4] E.J. McGuire, Phys. Rev. A 20 (1979) 445.
[5] W. Lotz, Z. Phys. 216 (1968) 241.
[6] Y.-K. Kim, M.E. Rudd, Phys. Rev. A 50 (1994) 3954.
[7] Y.-K. Kim, Phys. Rev. A 64 (2001) 032713.
[8] Y.-K. Kim, Phys. Rev. A 65 (2002) 022705.
[9] D.-H. Kwon, Y.-J. Rhee, Y.-K. Kim, Int. J. Mass Spectrom. 245 (2005) 26.
[10] Y.-K. Kim, P.M. Stone, Phys. Rev. A 64 (2001) 052707.
[11] Y.-K. Kim, J.P. Desclaux, Phys. Rev. A 66 (2002) 012708.
[12] W. Lotz, Z. Phys. 232 (1970) 101.
[13] W. Lotz, J. Opt. Soc. Am. 60 (1970) 206.
[14] See: http://physics.nist.gov/ionxsec.
[15] J.P. Desclaux, P. Indelicato, See: http://dirac.spectro.jussieu.fr/mcdf.
[16] Y.-K. Kim, M. Inokuti, Phys. Rev. A 3 (1971) 665.
[17] A.E. Kramida, T. Shirai, J. Phys. Chem. Ref. Data 35 (2006) 423.